Electronic supplementary information

Surface-controlled preparation of EuWO$_4$(OH) nanobelts and their hybrid with Au nanoparticles as a novel enzyme-free sensing platform towards hydrogen peroxide

Linglin Yu[a‡], Yao Wang[a‡], Qiong Wu[a‡], Ze Yuan[a], Xiaoji Xie[a], Zhiwei Wang[a], Ning Wang[a]*, Xiao Huang[a]*, Wei Huang[a]*

a. Key Laboratory of Flexible Electronics (KLOFE) & Institute of Advanced Materials (IAM), Jiangsu National Synergistic Innovation Center for Advanced Materials (SICAM), Nanjing Tech University (Nanjing Tech), 30 South Puzhu Road, Nanjing 211816, P.R. China.

Email: iamxhuang@njtech.edu.cn, iamnwang@njtech.edu.cn, wei-huang@njtech.edu.cn

1. Methods

1.1. Chemicals.

Ammonium metatungstate hydrate ((NH$_4$)$_{10}$H$_2$(W$_2$O$_7$)$_6$·xH$_2$O, 99.99%), thiourea (CS(NH$_2$)$_2$, ≥ 99.0%), sodium molybdate dihydrate (Na$_2$MoO$_4$·2H$_2$O, ≥ 99.0%), thioacetamide (CH$_3$CSNH$_2$, ≥ 99.0%), europium (III) nitrate hexahydrate (Eu(NO$_3$)$_3$·6H$_2$O, 99%), sodium citrate tribasic dehydrate (HOC(COONa)(CH$_2$COONa)$_2$·2H$_2$O, ≥ 99.0%), gold (III) chloride hydrate (HAuCl$_4$·xH$_2$O, 99.999%) were purchased from Sigma-Aldrich (Steinheim, Germany). H$_2$O$_2$ (30%) was purchased from Sinopharm Chemical Reagent Co., Ltd (Shanghai, China). Na$_2$HPO$_4$·12H$_2$O (≥ 99.0%), KH$_2$PO$_4$ (≥ 99.5%), Na$_2$CO$_3$ (≥ 99.8%), NaHCO$_3$ (≥ 99.5%), NaClO (≥ 5.2%) and HCl (36%) were purchased from Shanghai Linfeng Chemical Reagent Co., Ltd (Shanghai, China). Methylene blue (MB, 98.5%) was purchased from Tianjin Chemical Reagent Research Institute Co., Ltd (Tianjin, China). NaNO$_2$ (99.0%) and KNO$_3$ (99.0%) were purchased from Xilong Scientific Co., Ltd (Shantou, China). All reagents

were used as received without further purification. The deionized water was purified using a Milli-Q3 System (Millipore, France).

1.2. Synthesis of EuWO$_4$(OH) nanobelts.

In a typical process, 42 mg of $(NH_4)_{10}H_2(W_2O_7)_6 \cdot xH_2O$, 128 mg of $CS(NH_2)_2$ and 20 mg of $Eu(NO_3)_3 \cdot 6H_2O$ were dissolved in 19.5 mL distilled water in a 25 mL Teflon-lined stainless-steel autoclave. The autoclave was sealed and heated to 220 °C at 5 °C min^{-1} and maintained at this temperature for 24 h before cooled naturally to room temperature. The product was collected by centrifugation and washed with absolute ethanol and distilled water in turn before further characterizations.

1.3 Preparation of EuWO$_4$(OH)-Au hybrids.

0.04 mg of the EuWO$_4$(OH) nanobelt power was mixed with 9 mL aqueous solution containing 0.3 mM sodium citrate and 0.1 mM HAuCl$_4$ in a 10 mL glass bottle. Thereafter, the solution was irradiated with a 150 W halogen lamp at 70 % of its full intensity, during which the glass bottle was placed horizontally and kept 0.5 cm away from the light source. After 4 h of irradiation, the solution became red, indicating the formation of Au nanoparticles. The obtained product was then washed with water before further characterizations.

1.4 Characterizations.

The morphological, structural and compositional characterizations of the products were investigated by scanning electron microscopy (SEM, Hitachi S-4800, Japan), high resolution transmission electron microscope (HRTEM, JEOL 2100F, Japan) coupled with energy dispersive X-ray (EDX) spectroscopy, X-ray diffraction (XRD, SmartLab Rigaku, Japan), and X-ray photoelectron spectroscopy (XPS, PHI 5000 VersaProbe, Japan). The XRD characterization was carried on a diffractometer equipped with Cu K$_\alpha$ radiation (λ = 1.54 Å). For the XPS measurements, the binding energies were corrected for specimen

charging effects using the C 1s level at 284.6 eV as the reference. Excitation and emission spectra of the rare-earth compounds were measured under UV excitation at 250 nm on a fluorescent spectrometer (HitachiF-4600 FL) equipped with a power adjustable diode laser. The maximum photoluminescence of Eu^{3+} was recorded at 614 nm. Luminescence decay plots were obtained with a HORIBA Fluorolog-3 spectrofluorimeter under excitation at 250 nm. The pH values of buffer solutions were determined by a pH meter (Mettler Toledo Seven Excellent).

1.5 Investigation on the pH-dependent luminescence of EuWO₄(OH).

Buffer solutions were pre-prepared by mixing $Na_2HPO_4 \cdot 12H_2O$ and KH_2PO_4 (or Na_2CO_3 and $NaHCO_3$) at certain concentrations, and then their pH values were determined by a pH meter to be 6.0, 7.0, 8.0, 9.2, 10.1 and 10.8, respectively. To 2 mL of each of the above buffer solutions, 30 μL of $EuWO_4(OH)$ nanobelt dispersion in water (0.6 mg mL^{-1}) were added and incubated for 10 min at room temperature before their luminescent spectra were collected. All experiments were repeated three times, and the data were averaged.

1.6 Luminescent sensing of H₂O₂.

In a typical process, 2 mL of $EuWO_4(OH)$-Au (0.009 mg mL^{-1}) aqueous solution was mixed with 1 μL H_2O_2 aqueous solution with varied concentrations to give a final concentration of 0.1 to 3.0 μM in a quartz cuvette, followed by 8 min of incubation. After that, the emission intensity at 614 nm was recorded under 250 nm excitation. All experiments were repeated three times, and the data were averaged.

1.7 Production of various reactive oxygen species (ROS)

The various ROS were prepared based on previous report.[1] Nitrite (NO_2^-) was prepared from $NaNO_2$. Hypochlorite (OCl^-) was prepared from NaClO aqueous solution. Nitrate (NO_3^-) was prepared from an aqueous solution of $NaNO_3$. Peroxynitrite ($ONOO^-$) was prepared by mixing 0.6 M of $NaNO_2$ aqueous solution with 0.7 M H_2O_2 with the same

volume containing 0.6 M HCl.

1.8 Detection of hydroxyl radicals by using methylene blue (MB) as an indicator.

90 µL of sodium citrate aqueous solution (30 mM) and 30 µL of $HAuCl_4$ aqueous solution (30 mM) were mixed with 9 mL distilled water in a 10 mL glass bottle. Thereafter, the solution was irradiated with a 150 W halogen lamp at 70 % of its full intensity, during which the glass bottle was placed horizontally and kept 0.5 cm away from the light source. After 4 h of irradiation, the solution became red, indicating the formation of Au NPs. The obtained product was washed with water and then re-dispersed in 2 mLwater. 30 µL of this Au NP solution was mixed with 2 mL of MB (1.5 µM) aqueous solution in a quartz cuvette, into which 1 µL H_2O_2 aqueous solution (2 mM) was added to give a final concentration of 1.0 µM. UV-vis adsorption spectra of the solution were collected before and after H_2O_2 was added.
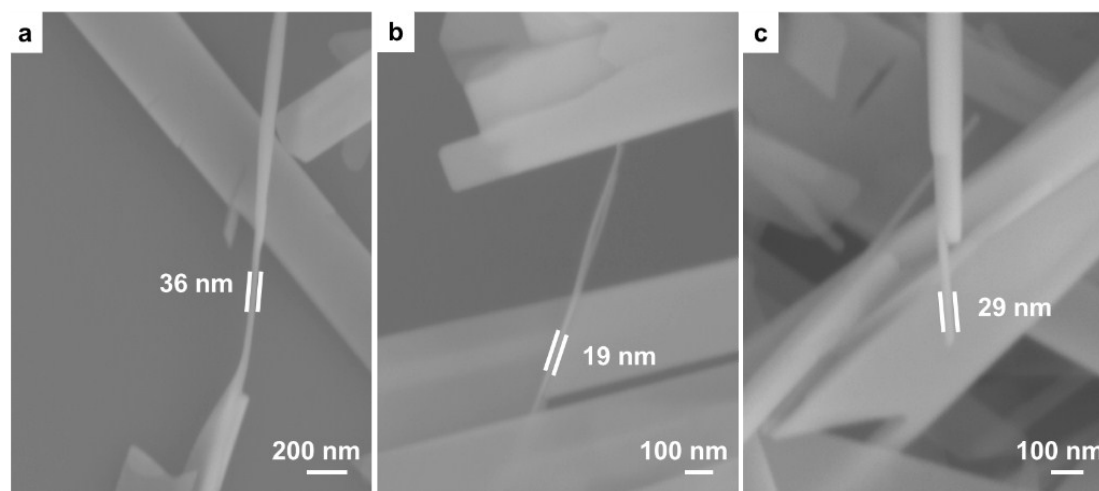

Fig. S1 Side-view SEM images of typical $EuWO_4(OH)$ nanobelts, revealing an average thickness of ~ 30 nm.
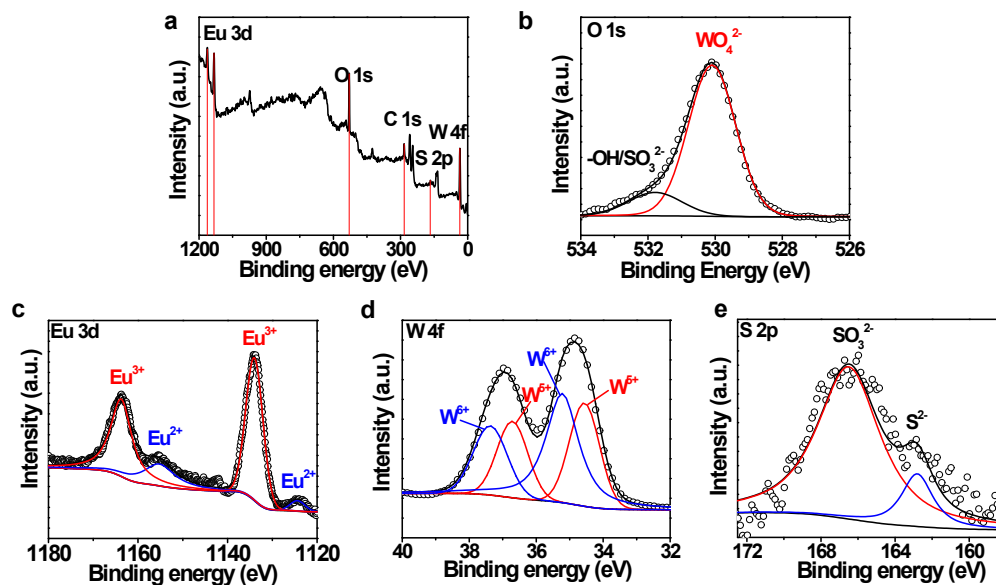
Fig. S2 XPS analysis of EuWO$_4$(OH) nanobelts. (a) Full scan, (b) O 1s, (c) Eu 3d, (d) W 4f and (e) S 2p spectra of the EuWO$_4$(OH) nanobelts deposited on Si/SiO$_x$.

As shown in **Fig. S2a**, Eu, W, S and O elements can be detected in the full scan spectrum. The high resolution O 1s spectrum in **Fig. S2b** can be deconvoluted to give two sets of doublet peaks, attributable to WO$_4^{2-}$ (530.08 eV) and –OH/SO$_3^{2-}$ (531.78 eV) species, respectively.[2] In the high resolution Eu 3d spectrum (**Fig. S2c**), two sets of doublet peaks can be assigned to Eu^{3+} (1134.00 and 1163.76 eV) and Eu^{2+} (1124.37 and 1155.20 eV) states, respectively.[3] The high resolution W 4f spectrum (**Fig. S2d**) reveals two sets of doublet peaks for W^{5+} (34.56 and 36.71eV) and W^{6+} (35.22 and 37.37 eV),[4] respectively. The high resolution S 2p spectrum (**Fig. S2e**) shows two peaks at 166.7 and 162.8 eV, assignable to SO$_3^{2-}$ and S^{2-}, respectively.[2, 5]
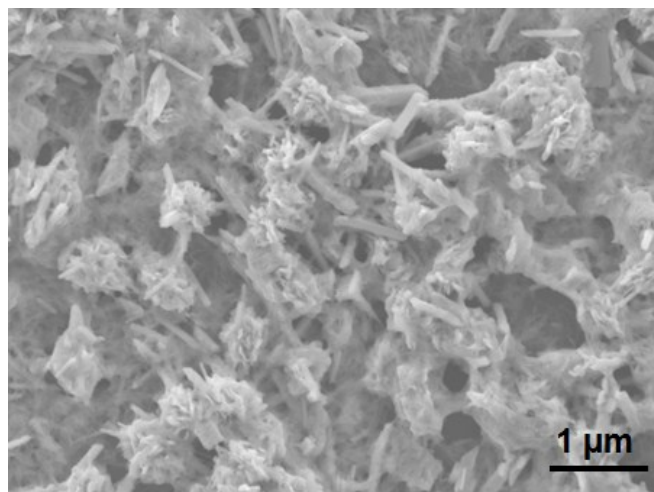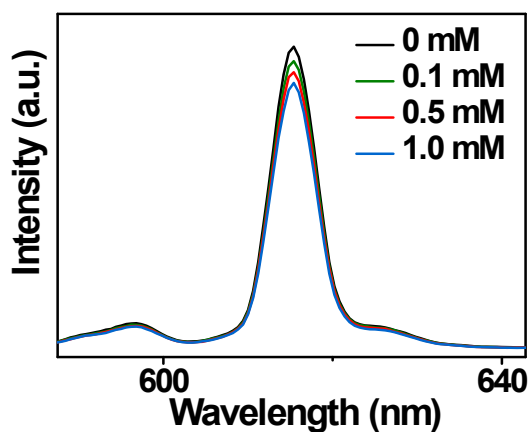
Fig. S3 SEM image of EuWO$_4$(OH) rods and irregular flower-like assemblies prepared without adding CS(NH$_2$)$_2$ to the synthetic solution.
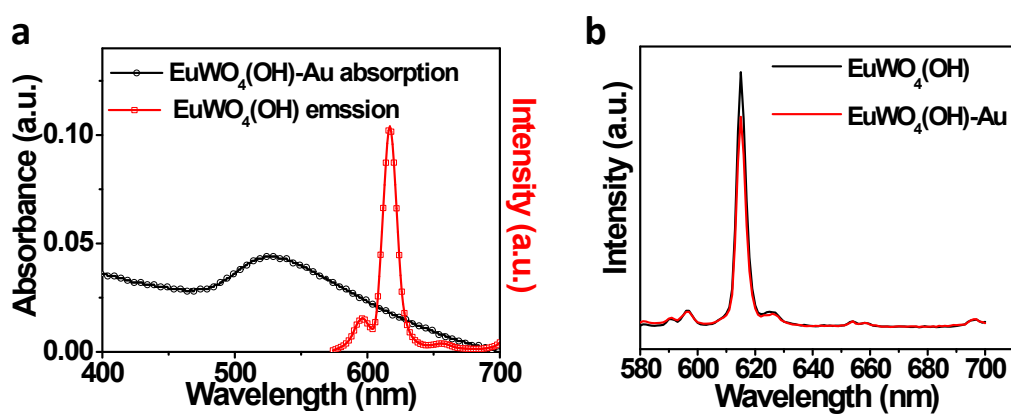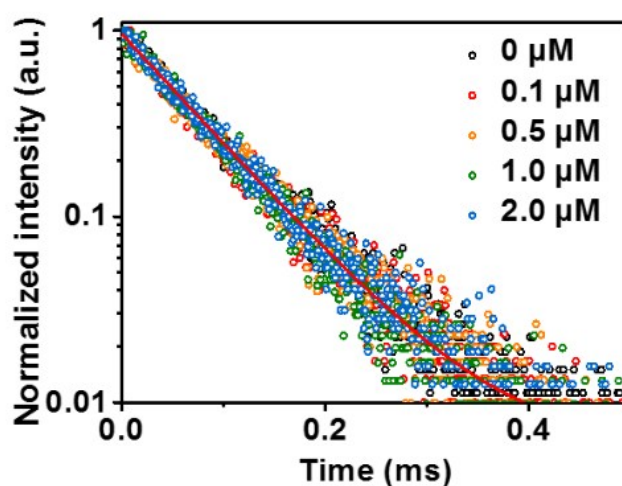

Fig. S4 (a) UV-vis absorption and luminescent emission spectra of EuWO$_4$(OH)-Au hybrid. The excitation wavelength is 250 nm. (b) Emission spectra of EuWO$_4$(OH) nanobelts and EuWO$_4$(OH)-Au hybrid upon excitation at 250 nm.
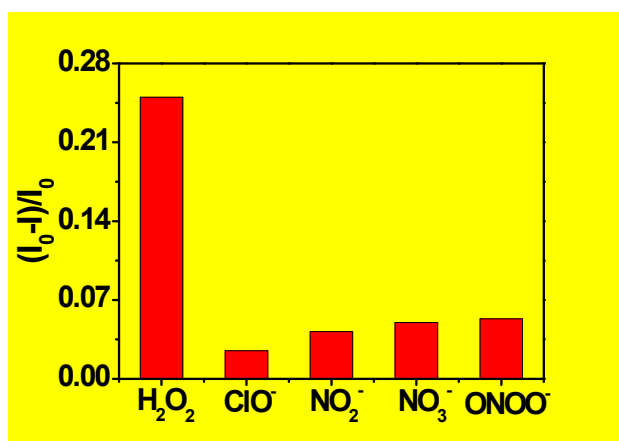
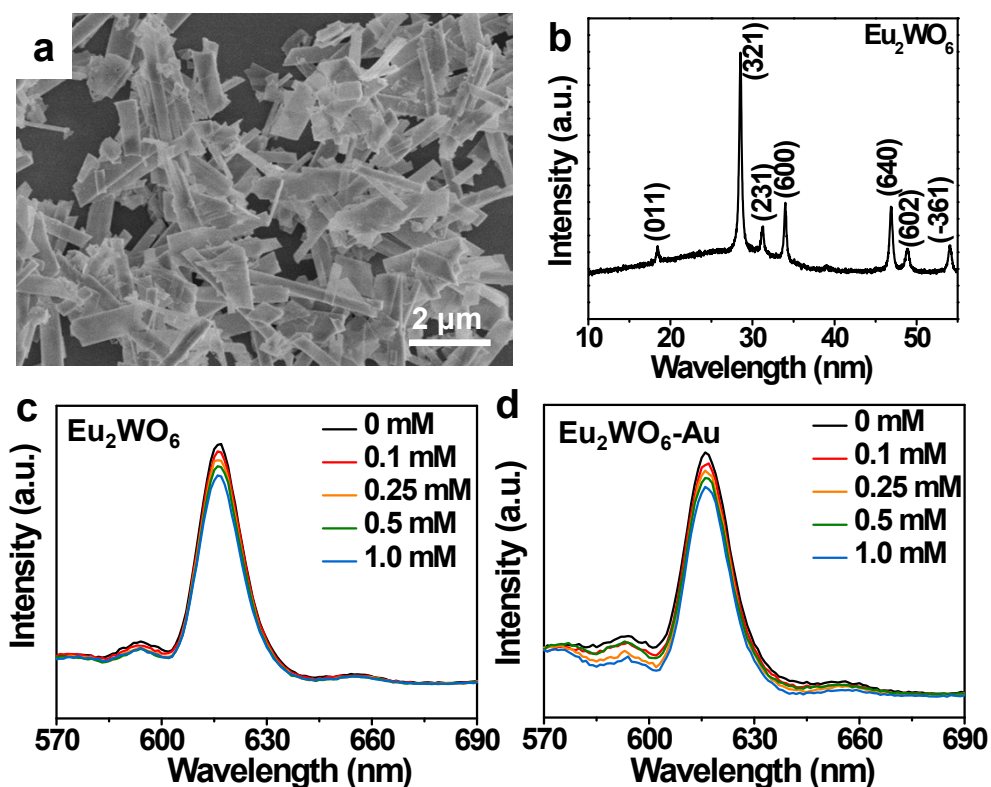**Fig. S6** Emission spectra of EuWO$_4$(OH) nanobelts in response to H$_2$O$_2$ with concentrations varying from 0.1 to 1.0 mM.

Fig. S7 Luminescence decay of the $^5D_0 \rightarrow ^7F_2$ transition of Eu^{3+} of EuWO$_4$(OH)-Au hybrid under the excitation at 250 nm in presence of H$_2$O$_2$ with different concentrations. Each set of the spots was fitted by a single exponential function.
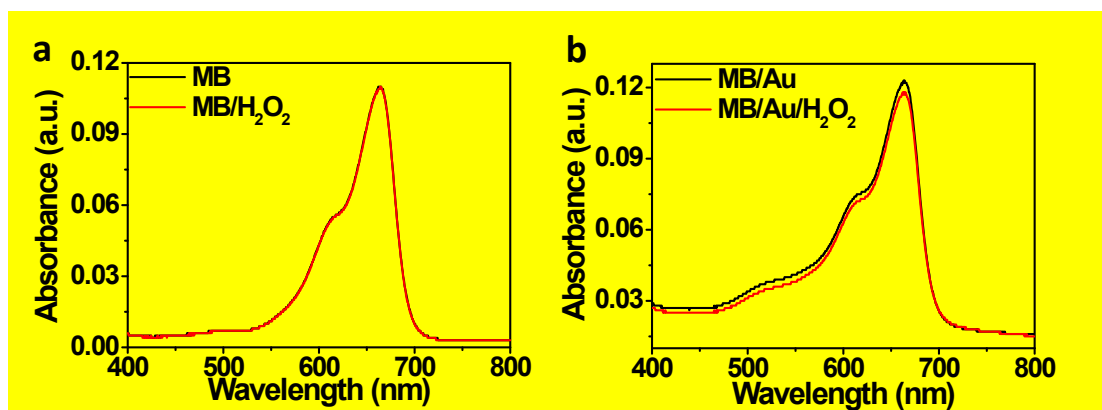
Fig. S8 (a) UV-vis absorption spectra of an MB (1.5 μM) solution before (black) and after (red) the addition of H_2O_2 (with a final concentration 1.0 μM). (b) UV-vis absorption spectra of a solution containing Au NPs and MB (1.5 μM) before (black) and after (red) the addition of H_2O_2 (with a final concentration of 1.0 μM).

Fig. S9 (a) SEM image and (b) XRD pattern of Eu_2WO_6 nanoplates obtained by heating $EuWO_4(OH)$ nanobelts in N_2 at 650 ºC for 2 h. PL spectra of (c) Eu_2WO_6 and (d) Eu_2WO_6-Au hybrid in presence of H_2O_2 with varying concentrations from 0-1.0 mM.

Table S1. Performance of various luminescent H_2O_2 sensors based on inorganic rare-earth nanocrystals.

Material	Linear range (M)	Limit of detection (nM)	Ref.
Eu(III)-doped $GdVO_4$ nanoparticles	5×10^{-6} to 2.5×10^{-4}	1600	6
$Y_{0.6}Eu_{0.4}VO_4$ nanoparticles	1×10^{-6} to 4.5×10^{-5}	/	7
YAG:Ce (4%) and $Gd_{0.6}Eu_{0.4}VO_4$ nanoparticles	5×10^{-7} to 1×10^{-5}	500	8
$(Y,Eu)PO_4$-$(Y,Eu)VO_4$ particles	1×10^{-2} to 4×10^{-1}	/	9
$EuVO_4$ nanoparticles	0-0.25 ppm	0.05 ppm	10
$EuVO_4$-based films	/	100 ppb	11
$NaYF_4$:Yb/Er upconversion nanoparticles	1×10^{-7} to 4×10^{-6}	45	12
(MnO_2)-nanosheet-modified upconversion nanoparticles	1×10^{-5} to 3.5×10^{-4}	900	13
CeO_2 nanoparticle	0 to 1×10^{-3}	130	14

1 (a) M. H. Lan, Y. F. Di, X. Y. Zhu, T.-W. Ng, J. Xia, W. M. Liu, X. M. Meng, P. F. Wang, C.-S. Lee and W. J. Zhang, *Chem. Commun.*, 2015, **51**, 15574; (b) Z. N. Sun, H. L. Wang, F. Q. Liu, Y. Chen, P. K. Tam and D. Yang, *Org. Lett.*, 2009, **11**, 1887.

2 Y. S. Liu, D. T. Tu, H. M. Zhu, R. F. Li, W. Q. Luo and X. Y. Chen, *Adv. Mater.*, 2010, **22**, 3266.

3 (a) V. G. Pol, O. Palchik, A. Gedanken and I. Felner, *J. Phys. Chem. B*, 2002, **106**, 9737; (b) B. Z. Zhao, X. J. Xie, S. L. Xu, Y. Pan, B. X. Yang, S. H. Guo, T. Wei, H. Q. Su, H. B. Wang, X. Q. Chen, V. P. Dravid, L. Huang and W. Huang, *Adv. Mater.*, 2016, **28**, 6665.

4 K. Oka, T. Nishiguchi, H. Kanai, K. Utani and S. Imamura, *Appl. Catal. A-Gen.*, 2006, **309**, 187.

5 (a) Z. Z. Li, Y. M. Xin, W. L. Wu, B. H. Fu and Z. H. Zhang, *Anal. Chem.*, 2016, **88**, 7724; (b) G. M. Bremmer, L. van Haandel, E. J. M. Hensen, J. W. M. Frenken and P. J. Kooyman, *J. Phys. Chem. C*, 2016, **120**, 19204.

6 V. Muhr, M. Buchner, T. Hirsch, D. J. Jovanović, S. D. Dolić, M. D. Dramićanin and O. S. Wolfbeis, *Sensor Actuat. B: Chem.*, 2017, **241**, 349.

7 D. Casanova, C. Bouzigues, T. L. Nguyen, R. O. Ramodiharilafy, L. Bouzhir-Sima, T. Gacoin, J. P. Boilot, P. L. Tharaux and A. Alexandrou, *Nat. Nanotechnol.*, 2009, **4**, 581.

8 M. Abdesselem, R. Ramodiharilafy, L. Devys, T. Gacoin, A. Alexandrou and C. I. Bouzigues, *Nanoscale*, 2017, **9**, 656.

9 P. C. de Sousa Filho, E. Larquet, D. Dragoe, O. A. Serra and T. Gacoin, *ACS Appl. Mater. Interfaces*, 2016.

10 N. Duée, C. Ambard, F. Pereira, D. Portehault, B. Viana, K. Vallé, D. Autissier and C. Sanchez,

Chem. Mater., 2015, **27**, 5198.

11   C. Ambard, N. Duée, F. Pereira, D. Portehault, C. Méthivier, C.-M. Pradier and C. Sanchez, *J. Sol-Gel Sci. Technol.*, 2016, **79**, 381.

12   J. Liu, L. Lu, A. Li, J. Tang, S. Wang, S. Xu and L. Wang, *Biosens. Bioelectron.* , 2015, **68**, 204.

13   J. Yuan, Y. Cen, X. J. Kong, S. Wu, C. L. Liu, R. Q. Yu and X. Chu, *ACS Appl. Mater. Interfaces*, 2015, **7**, 10548.

14   B. Liu, Z. Sun, P. J. Huang and J. Liu, *J. Am. Chem. Soc.*, 2015, **137**, 1290.